



# **IR transparent Y<sub>2</sub>O<sub>3</sub>-MgO nanocomposite ceramic processed by sol-gel synthesis and two-step SPS sintering**

Nathan Brard, Johan Petit, Benjamin Villeroy, Stéphane Bach

## **► To cite this version:**

Nathan Brard, Johan Petit, Benjamin Villeroy, Stéphane Bach. IR transparent Y<sub>2</sub>O<sub>3</sub>-MgO nanocomposite ceramic processed by sol-gel synthesis and two-step SPS sintering. SPIE Defense + Commercial Sensing, Apr 2023, Orlando, United States. <10.1117/12.2663490>. <hal-04150068>

**HAL Id: hal-04150068**

**<https://hal.science/hal-04150068v1>**

Submitted on 4 Jul 2023

**HAL** is a multi-disciplinary open access archive for the deposit and dissemination of scientific research documents, whether they are published or not. The documents may come from teaching and research institutions in France or abroad, or from public or private research centers.

L'archive ouverte pluridisciplinaire **HAL**, est destinée au dépôt et à la diffusion de documents scientifiques de niveau recherche, publiés ou non, émanant des établissements d'enseignement et de recherche français ou étrangers, des laboratoires publics ou privés.



HAL Authorization

# IR transparent Y<sub>2</sub>O<sub>3</sub>-MgO nanocomposite ceramic processed by sol-gel synthesis and two-step SPS sintering

Nathan Brard<sup>\*ab</sup>, Johan Petit<sup>a</sup>, Benjamin Villeroy<sup>b</sup>, Stéphane Bach<sup>bc</sup>

a DMAS, ONERA, Université Paris Saclay F-92322 Châtillon – France

b ICMPE, CNRS, UMR 7182, 2 Rue Henri Dunant, 94320 Thiais, France

c Université Paris Saclay - Evry, Dept Chimie, Bd F. Mitterrand, 91000 Evry, France

## ABSTRACT

Transparent ceramics are materials of choice for high temperature IR window applications: they are a compromise between transparency, thermal shock resistance and processing costs. Alumina, AlON and spinel-type ceramics have been developed for the 3-5  $\mu\text{m}$  atmospheric transparency band. Nevertheless, these compounds show a degradation of their optical properties (transparency and emissivity) at high temperature (above 500°C), limiting their use in that wavelength range. MgO and Y<sub>2</sub>O<sub>3</sub> have a broader transparency window up to 9  $\mu\text{m}$  and they are transparent enough in the 3-5  $\mu\text{m}$  range even at high temperature but their thermomechanical resistance is weak. Authors have combined these compounds into a nanocomposite ceramic to improve this while keeping good IR transparency. To reach such properties, porosity ratio must be close to zero and the average grain size must stay as small as possible (< 200 nm).

Throughout this study, Pechini's esterification sol-gel route was chosen in order to process the Y<sub>2</sub>O<sub>3</sub>-MgO nanocomposite powder. Then, a two-step sintering and low temperature profiles (700°C) were performed by the Spark Plasma Sintering technique. Post treatments, air annealing and Hot Isostatic Pressing at 400MPa, improved the quality of the ceramics. Finally, structural, microstructural and optical characterizations were carried out. Samples with different nanostructures were obtained. The best samples have average grain diameters below 200 nm with almost no porosity. Good mid-IR transparency, up to 80% for a thickness of 1 mm, was obtained in band II. The material showed a loss of transparency at 5 $\mu\text{m}$  below 15% at 1000°C.

**Keywords:** Y<sub>2</sub>O<sub>3</sub>-MgO nanocomposites, SPS, two-step sintering, sol-gel synthesis, IR transparent ceramic

## 1 INTRODUCTION

In the last twenty years, MgO-Y<sub>2</sub>O<sub>3</sub> transparent nanocomposite ceramics have been developed to be used as high temperature infrared (IR) windows for wavelengths between 3 to 5  $\mu\text{m}$  (band II) [1]–[3]. Indeed, even if conventional IR transparent ceramics such as alumina, AlON, spinel are good materials for transparency in the 3-5  $\mu\text{m}$  band at room temperature, their transparency windows go up to around 6  $\mu\text{m}$  and are limited for high temperature applications (1000°C) [4], [5]. It is due to the increase of the multiphonon absorption when temperature rises. This is also correlated to the increase of the emittance of the material, which leads to a degradation of its optical properties. It is thus a challenge to keep a sufficient IR transparency in the band II at high temperature (1000°C). One of the options is to use a material with a broader window.

The ceramic studied in this paper is a composite made with yttria and magnesia, both immiscible up to 2110 °C. MgO and Y<sub>2</sub>O<sub>3</sub> are two transparent ceramics with a transparency window up to 9  $\mu\text{m}$  [5] but their thermomechanical resistance are too weak when tested separately to be used in a harsh environment. By combining these compounds, it is possible to slow down the granular growth and obtain a nanostructure more easily. The final nanocomposite MgO-Y<sub>2</sub>O<sub>3</sub> has comparable IR optical properties as MgO and Y<sub>2</sub>O<sub>3</sub> and better thermomechanical properties enhanced by nanoscale grains [2]. In order to achieve the desired properties, it is important to minimize the porosity ratio close to zero and ensure that the microstructure is as uniform as possible. Additionally, it is necessary to keep the average grain size as small as possible (less than 200 nm) to mitigate scattering at grain boundaries resulting from the refractive index difference between MgO and Y<sub>2</sub>O<sub>3</sub>, and to enhance the material's mechanical properties.

Many studies have already developed MgO-Y<sub>2</sub>O<sub>3</sub> nanocomposite ceramics by varying the powder synthesis, sintering, and post-treatment processes. Materials with dense and homogeneous microstructures, and grain sizes smaller than 100 nm have been obtained [3]. It is possible to achieve transmittances greater than 80% for a thickness of 2 mm between 3 and 5  $\mu$ m wavelengths. In a recent paper, we have shown that the transparency of this nanocomposite ceramic in the IR band II remains weakly impacted even up to 1000°C [6]. The thermomechanical properties are also superior to those of separate magnesia and yttria, approaching those of commercial materials [2].

In this study, MgO-Y<sub>2</sub>O<sub>3</sub> nanocomposite ceramic materials were developed. A nanocomposite powder was synthesized via the sol-gel route before being sintered by Spark Plasma Sintering (SPS). This sintering was then coupled with Hot Isostatic Pressing (HIP), available at ONERA and which goes up to 400 MPa, in order to densify the ceramic as much as possible. In addition to the use of HIP up to 400 MPa, the originality of this work lies in two different heat treatments: sintering at temperatures below 1000°C—which, to our knowledge, has never been achieved in the literature—as well as a new two-step sintering process described in a recent publication [6]. This latter type of heat treatment has already been shown to favor densification mechanisms by limiting those related to grain growth [7]–[9]. Firstly, a comparison of different heat treatments for SPS sintering will be presented. Then, some effects of post-treatments (HIP and annealing under air) on the microstructure of the materials and their transparency properties will be described.

## 2 EXPERIMENTAL APPROACH

### 2.1 Powder synthesis

The nanocomposite powder of MgO and Y<sub>2</sub>O<sub>3</sub> was synthesized following the experimental protocol presented in our previous work [6]. An aqueous solution composed by magnesium nitrate hexahydrate (Mg (NO<sub>3</sub>)<sub>2</sub>·6H<sub>2</sub>O, 99.5%), yttrium nitrate hexahydrate (Y(NO<sub>3</sub>)<sub>3</sub>·6H<sub>2</sub>O, 99.5%), citric acid monohydrate (C<sub>6</sub>H<sub>8</sub>O<sub>7</sub>·H<sub>2</sub>O, 99.5%) and ethylene glycol (C<sub>2</sub>H<sub>6</sub>O<sub>2</sub>, 99%) was heated in an alumina crucible up to 800°C, to obtain the powder through a sol-gel route. The powder was then sieved and stored in an oven at 150°C. The temperature of 800°C was chosen to avoid organic remains in the powder and to limit the diameter of the grains as much as possible. The proportion of precursors was selected to obtain a volume ration of 50:50 between MgO and Y<sub>2</sub>O<sub>3</sub> in the final sintered samples.

### 2.2 Sintering and post-treatments

The powder was then put into a graphite die to sinter it using using a Dr. Sinter 515S Syntex setup belonging to the "Plateforme de Frittage Ile de France" (Thiais, France) that allowed us to make pellets with a 15 mm diameter and a 3 mm thickness (after sintering). One layer of 0.15 mm thick graphite paper provided electric and thermal contacts between rams, powder and mold. Two thermal profiles under vacuum have been used for sintering and are presented in the Figure 1. In both, a pre-sintering dwell of 5 min at 650°C was applied before reaching the sintering temperature, the pressure was increased at this moment from 10 MPa to the sintering pressure. The sintering temperatures, ramps' speed, bearing times and pressures applied will be specified later. The first thermal profile, referred as "one-step", was composed of a simple step, of 10 min in this study, at the sintering temperature. Few one-step sintering were carried out at lower temperatures, under 1000°C, than in the literature. The second thermal profile, referred as "two-step", was composed of a classical dwell at the sintering temperature preceded by a rapid cooling to room temperature after reaching the sintering temperature without bearing time. During the rapid cooling, argon was introduced into the chamber to cool down faster. The vacuum was again made at room temperature. The temperatures were measured with a thermocouple, placed in a hole in the side of the die, for sintering under 1000°C and with a pyrometer focusing on this same hole for higher temperatures.

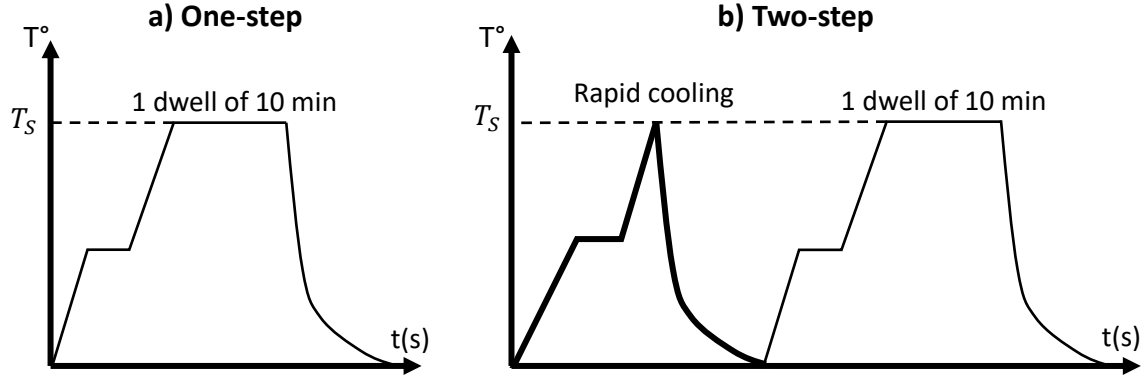


Figure 1. Thermal profiles for the SPS process: a) with “one-step” b) with “two-step” showing in bold the previous additional step.

Sintered samples were then Hot Isostatically Pressed (HIP) at 1200°C under 400 MPa for 2h. Then, samples were air annealed in a muffle furnace for 40 or 100h at 1000°C. Finally, a polishing down to 1/4  $\mu\text{m}$  was carried out prior to their characterizations.

### 2.3 Characterizations

Densities of the sintered samples were evaluated with the Archimedes’ method (accuracy around 1%), assuming a density of 4.293 g/cm<sup>3</sup> for the 50:50 vol% composite. Nanocomposites were cut and polished before collecting Scanning Electron Microscopy (SEM) pictures to study their microstructures. The average grain size was determined using the intercept method with a coefficient of 1.56. A Fourier Transform IR spectrophotometer was used to determine the near and the mid infrared transmittance of the samples. Transmission curves were measured on samples of a given thickness and then re-calculated to correspond to the desired comparison thickness as explained in our previous work [6]. Finally, the high-temperature transmission measurements were carried out using a specific IR scanning spectrophotometer assembled at ONERA. The sample was heated in a chamber at temperatures ranging from 20 to 1000°C. Measurements were made using a monochromator, a lock in amplifier, anti-reflected ZnSe optics, an IR lamp, several long-pass filters from 3 to 9  $\mu\text{m}$  and a 77K cooled MCT detector.

## 3 SPS SINTERING

### 3.1 Sintered samples

All the sintering conditions developed in this study are summed up in the Figure 2. Table 1 and the Figure 2 shows the photography of all the samples excepted 2B. One-step sintering has been done by varying the sintering temperature from 700°C (1A) to 1500°C (1E). Samples 1A and 1B are sintered at lower temperatures than the ones found in the literature. The idea of sintering at this temperature came from the value of the SPS ram displacement that was ended around 800°C. Unlike the other samples, they appear grey in volume because of the higher amount of impurities coming from the powder. A higher temperature allows the release of these impurities. Moreover, these samples are cracked at the edges but globally intact. Above 1000°C, samples are split in two. The two-step sintered sample (2A) is intact and shows a grey surface, which is a part of the graphite paper. The sample 2B, processed at a lower pressure, will not be presented in this part but in the part 4. Its IR transparency after post-treatments will be discussed.

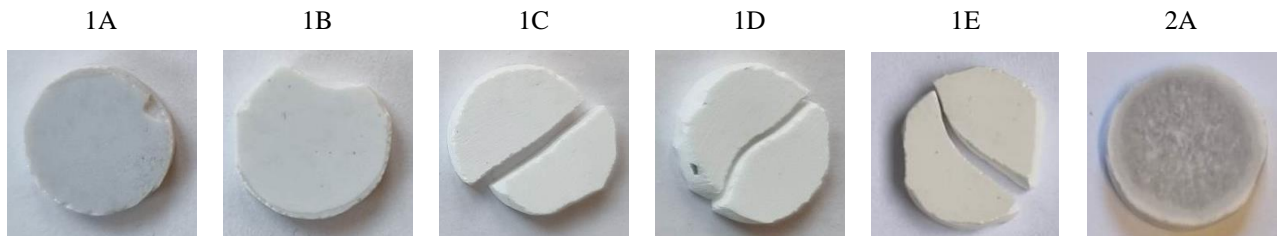


Figure 2. Pictures of the MgO-Y<sub>2</sub>O<sub>3</sub> nanocomposite samples processed by SPS.

Table 1. Summary of the sintering conditions of the MgO-Y<sub>2</sub>O<sub>3</sub> nanocomposite samples processed by SPS.

Sample	Thermal treatment	Sintering temperature (°C)	Temperature rising rate (°C/min)	Bearing time (min)	Pressure (MPa)
1A	One-step – low T°	700	100	10	70
1B	One-step – low T°	800	100	10	70
1C	One-step	1000	100	10	70
1D	One-step	1200	100	10	70
1E	One-step	1500	100	10	70
2A	Two-step	1200	200	10	70
2B	Two-step	1200	200	10	50

### 3.2 Microstructures

These various thermal treatments have a significant effect on the samples' microstructure. The latter are visible in the SEM pictures of the Figure 3. Figure 4 gives the mean grain size (a) and the porosity ratio (b) of the MgO-Y<sub>2</sub>O<sub>3</sub> samples presented above.

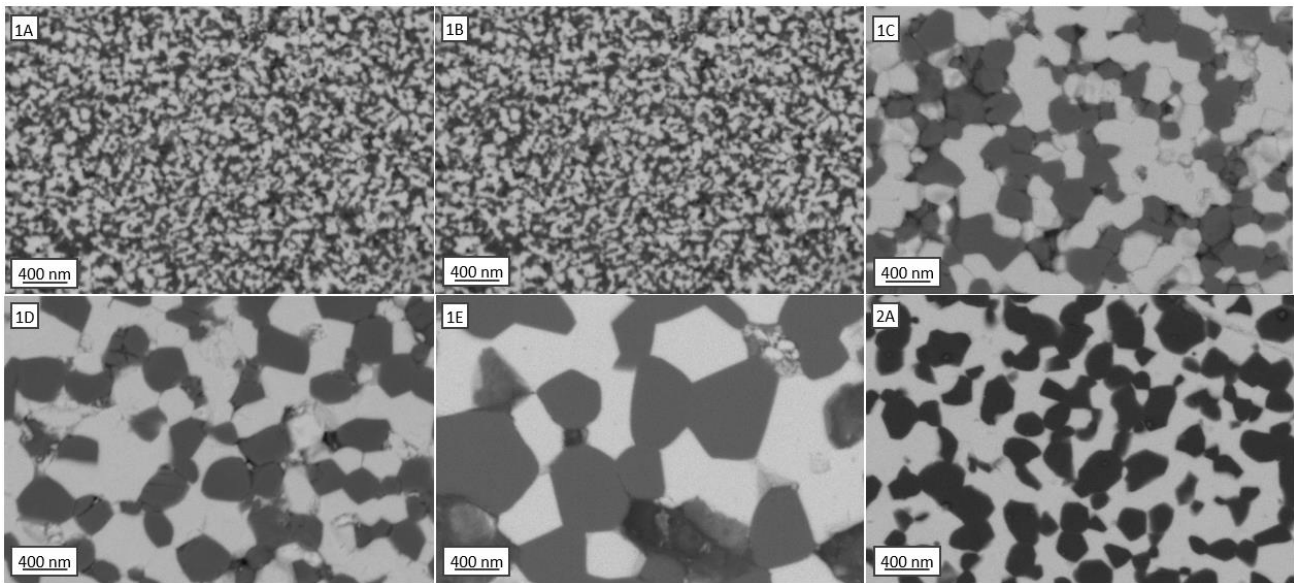


Figure 3. SEM pictures (BSE) showing the microstructures (light: yttria; dark: magnesia) of MgO-Y<sub>2</sub>O<sub>3</sub> nanocomposite samples sintered by SPS from a sol-gel powder synthesized at 800°C. Except the sample 2A, which was two-step, sintered at 1200°C, the other samples were one-step sintered at different temperatures. 1A: 700°C, 1B: 800°C, 1C: 1000°C, 1D: 1200°C, 1E: 1500°C.

By observing the one-step sintered samples at conventional temperatures (1C, 1D, 1E), an increase in the grain diameter with temperature is clearly visible. The energy given to the system by the increase in temperature amplifies the grain growth. However, the densification mechanisms do not seem to be activated enough, since the porosity ratio remains above 6%, which is too high for an infrared transmission. It also seems to be an increase of the porosity ratio when temperature rises, from 7% for a sample sintered at 1000°C to 17% for a sample sintered at 1500°C. As the powder used is hygroscopic and may still contain organic residue from the sol-gel route, this phenomenon could be explained by the release of different gas molecules [10]. On the microstructures presented in the Figure 3, there are nanopores at the grain boundaries.

With a sintering at a lower temperature, (1A and 1B) microstructures become much finer. For 10 min at 700°C, the mean grain size stays around 70 nm. As grain size affects the grain boundary optical scattering, reducing this value under 100 nm is interesting to consider transparency in the visible wavelengths. Furthermore, the porosity ratio is still significant. On the Figure 3, the grains inside both samples 1A and 1B appear more interlocked. This microstructure may result less from atomic diffusion than from plastic deformation under load, regarding the relatively low temperature, allowing the samples

to be compacted. This could be due to the characteristics of our nanometric powder that may have an amorphous phase ratio. Further experiments will be conducted to gain more insight.

Finally, the two-step sintering, with the same sintering temperature and time, reduces the grain size and improves the density of the nanocomposite. For a sintering temperature of 1200°C, the mean grain size is reduced from 430 nm (one-step) to 230 nm (two-step) and the porosity ratio decreases to 3%. The change in the thermal history of the sample, here the rapid cooling, favors densification over grain growth. This could be explained by the establishing of a special network of grain boundaries that reduces the driving force of the grain growth [8].

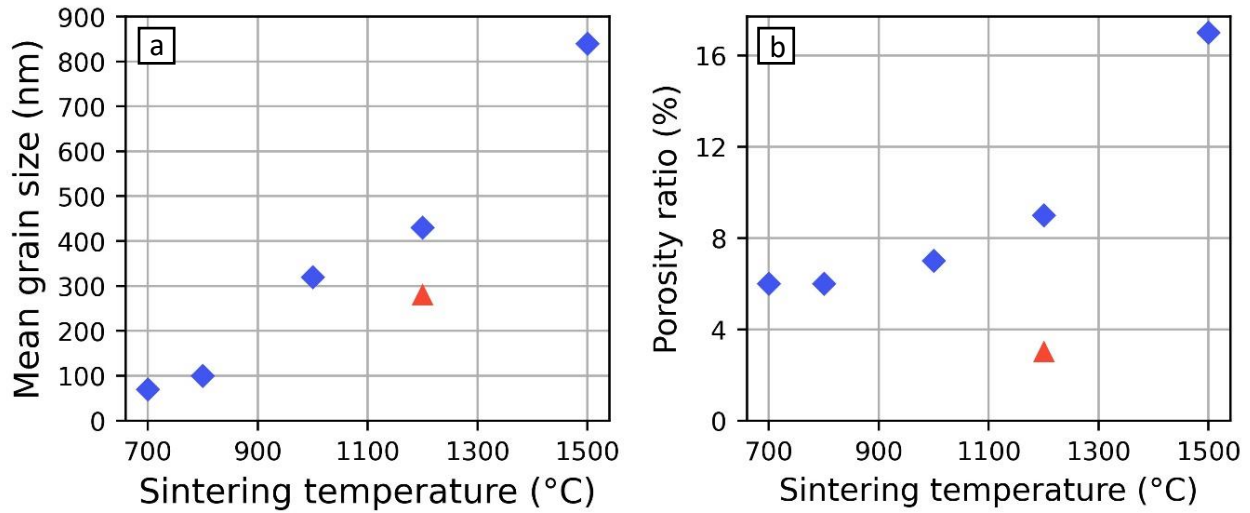


Figure 4. Evolution of the mean grain size in nm (a) and the porosity ratio in percentage (b) of the MgO-Y<sub>2</sub>O<sub>3</sub> nanocomposite samples sintered by SPS versus the sintering temperature. Blue ♦: One-step sintered samples. Red ▲: Two-step sintered samples.

### 3.3 Optical properties

The Figure 5 shows the transmittance of the samples in the near and mid-infrared.

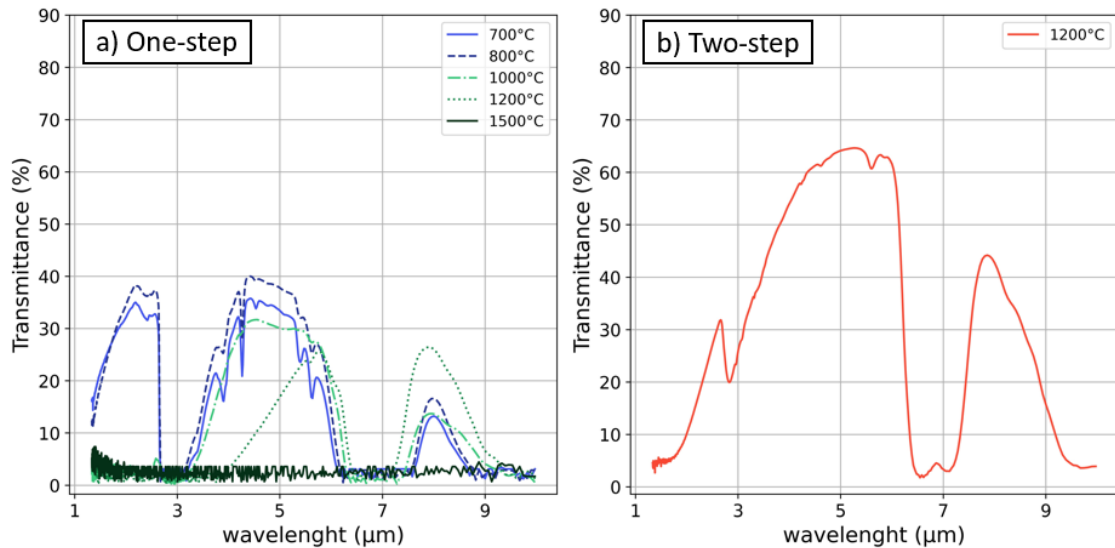


Figure 5. Infrared transmission of MgO-Y<sub>2</sub>O<sub>3</sub> nanocomposites after SPS sintering obtained on a 2 to 3 mm sample and then calculated for a thickness of 1 mm. a) Samples sintered in one step. b) Samples sintered in two steps.

The overall transmittance of the one-step sintered samples (Figure 5a) does not exceed 40% for a thickness of 1 mm. This result was expected due to the low density of the samples. Moreover, the higher the sintering temperature, the higher the porosity and the lower the overall transparency of the sample. It even reaches zero for the sample 1E, sintered at 1500°C with a porosity ratio of 17%. The sample 2A (Figure 5a), two-step sintered, was denser. Its overall transparency exceeds 60% at 5  $\mu\text{m}$ . However, pores are not the only cause of light scattering. Grain boundaries too. Scattering at grain boundaries is more significant for larger grain sizes and reduces transparency for shorter wavelengths. The samples 1A and 1B, which have the smallest average grain diameters, clearly exhibit the highest transmittance between 1 and 2.5  $\mu\text{m}$  wavelengths. Otherwise, two absorption bands are observed. One at 7  $\mu\text{m}$  results from the vibration of carboxyl groups due to contamination during the SPS process and the sol-gel synthesized powder [11]. The second, around 3  $\mu\text{m}$ , is related to hydroxyl groups. Finally, the samples sintered at lower temperatures, 700 and 800°C, exhibit several other absorption peaks related to impurities in the powder and their hydroxyl groups absorption band at 3  $\mu\text{m}$  is also very significant and causes the transmittance to tend towards zero.

## 4 POST-TREATMENTS

### 4.1 Post treated samples

Post-treatments are an important part of the process. Hot isostatic pressing allows reaching appropriate densification to obtain a transparent sample. With air annealing, it is possible to restore the oxygen stoichiometry, which improves the transparency [12], and releases some impurities such as moisture. Next, 40h air annealing at 1000°C impact on the one-step sintered samples is evaluated. Then, the optical properties of the two-step sintered (2B) and post-treated (HIP and air annealing) MgO-Y<sub>2</sub>O<sub>3</sub> nanocomposite sample presented in our previous work [6], in similar conditions to the previous ones, is characterized until 1000°C for a broader wavelength window (from 4  $\mu\text{m}$ ). The samples and their post-treatments are summarized in Table 2. As some samples are cracked, the porosity ratio is not evaluated.

Table 2. Summary of the different MgO-Y<sub>2</sub>O<sub>3</sub> post-treated nanocomposite samples. Mean grain size (intercept method with 1.56 ratio) and porosity ratio (Archimedes method) are given. Air annealing was processed at 1000°C and HIP at 1200°C under 400 MPa.

Sample	Original sample	Post treatment	State	Mean grain size (nm)	
				Before	After
1A*	1A	Air annealing (40h)	cracked	70	130
1B*	1B	Air annealing (40h)	cracked	100	130
1C*	1C	Air annealing (40h)	intact	320	310
D*	1D	Air annealing (40h)	intact	430	390
2B <sup>H</sup>	2B	HIP (2h)	intact	150	220
2B <sup>H*</sup>	2B <sup>H</sup>	HIP (2h) + air annealing (100h)	intact	220	240

### 4.2 One-step sintered samples

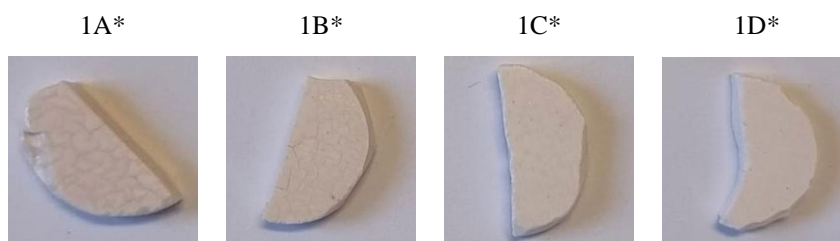


Figure 6. Pictures of the different MgO-Y<sub>2</sub>O<sub>3</sub> nanocomposite sample one-step sintered by SPS after air annealing for 40h.

The Figure 6 shows the photos of the samples after annealing in air. As presented in Table 2, the samples initially sintered at lower temperatures (1A: 700°C and 1B: 800°C) came out of the furnace cracked (1A\* and 1B\*). These cracks can be explained by the evaporation of impurities or moisture that were initially present in the powder and had not been released during sintering due to the low temperatures. While annealing may seem like a solution to improve the transparency of the samples, which exhibit numerous absorption peaks related to impurities, a broken sample presents no

interest. Additional results with milder annealing conditions, i.e. slower temperature ramp rates, are planned. The nanocomposites produced at temperatures above 1000°C, on the other hand, do not exhibit any cracks.

Figure 7 shows SEM images of the microstructures of these air annealed samples. It appears that the 1000°C treatment induced grain growth for samples 1A\* and 1B\*. Their mean grain size raises respectively from 70 and 100 nm to 130 nm (Table 2). However, the grain size of the two other samples (1C\* and 1D\*) decreases slightly, which seems impossible. The error bar on the measurement requires us to conclude that these results are not significant but are to keep in mind.

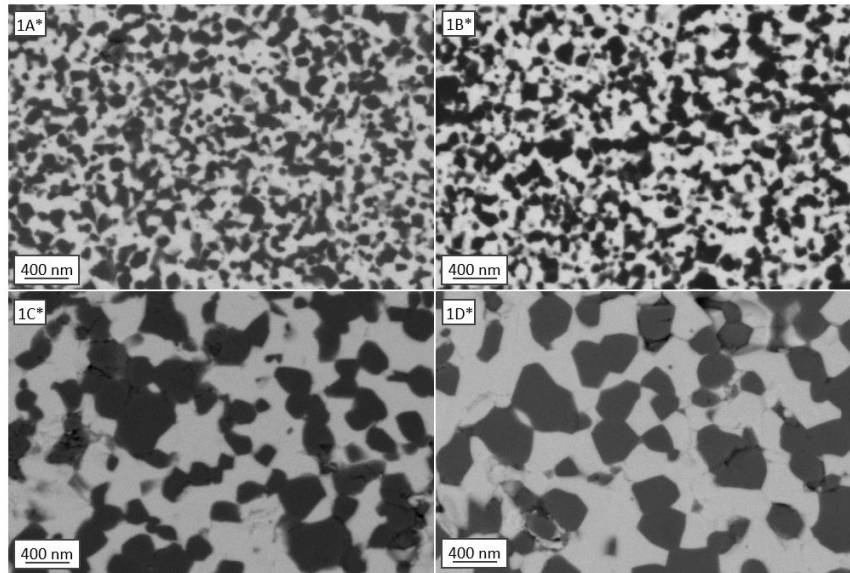


Figure 7. SEM pictures (BSE) showing the microstructures (light: yttria; dark: magnesia) of MgO–Y<sub>2</sub>O<sub>3</sub> nanocomposite samples sintered by SPS and air annealed 40h. The samples were initially one-step sintered at different temperatures. 1A: 700°C, 1B: 800°C, 1C: 1000°C, 1D: 1200°C.

#### 4.3 Two-step sintered samples

The figure below (Figure 8) presents the optical transparency properties after post-treatment of the sample 2B, sintered during a previous study [6]. This sample initially had a denser microstructure (porosity rate < 1%) and a finer one (150 nm). As shown in Figure 8a, post-treatments improve the IR transparency of the nanocomposite. The overall transparency is increased after HIP because of the densification of the material. Then, the restoration of oxygen vacancies and the release of water trapped in the material during the air annealing improved overall transparency and attenuated the absorption band at 3  $\mu$ m. However, none of the post-treatments could attenuate the absorption peak at 7  $\mu$ m. As the latter is not in the wavelength range of interest, it is not a significant problem.

Next, the transmission up to 1000°C was measured (Figure 8b) from 4 to 9  $\mu$ m in wavelength. The purpose of this figure is to analyze the impact of temperature on the evolution of transparency. Unlike in the Figure 8a, transmittance is calculated for a thickness of 2 mm. Due to the increase of absorption at high temperatures, transparency window of the nanocomposite reduces as expected at the higher wavelengths. As the transparency window goes up to 9  $\mu$ m at room temperature, the transmittance at 5  $\mu$ m starts only to decrease from 750°C. At 1000°C, the loss of transmittance for the wavelength of 5  $\mu$ m is about 15%. The effects of the reducing environment of the IR scanning spectrophotometer, which contains graphite parts, must be taken into account in this decrease. As it can be seen, the transmittance at room temperature after the characterization does not return to its initial value. Finally, there is no real change in transparency at 4  $\mu$ m.



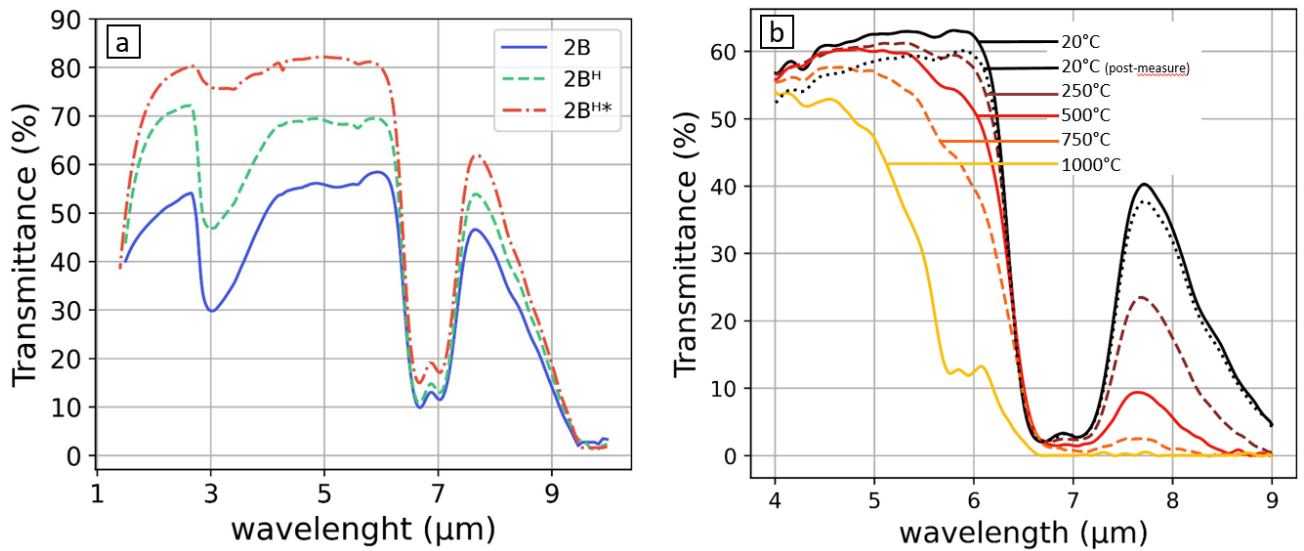


Figure 8. IR transmission of a MgO-Y<sub>2</sub>O<sub>3</sub> nanocomposite. The sample (2B) was two-step sintered from a sol-gel powder synthesized at 800°C. The sample was then HIP (1200°C for 2h under 400 MPa) before annealing under air (1000°C for 100h). a: IR transmission at room temperature for a thickness of 1 mm. (2B : Post-SPS, 2B<sup>H</sup> : after HIP and 2B<sup>H\*</sup>: after HIP + air annealing). b: IR transmission of the sample 2B<sup>H\*</sup> up to 1000°C for a thickness of 2 mm.

## 5 CONCLUSION

In conclusion, MgO-Y<sub>2</sub>O<sub>3</sub> nanocomposite ceramic materials were obtained from sol-gel nanometric powders and composites synthesized at 800°C. SPS sintering was carried out by studying different heat treatments. Samples were obtained by sintering at 700 and 800°C, which is much lower than conventional temperatures for this material, which are usually above 1000°C. Sintering at such a low temperature allows for a finer microstructure without increasing the pressure too much: 70 nm for sintering at 700°C and 70 MPa. And the porosity ratio remains quite low in comparison with sample treated at higher temperatures. However, it is still too high, and moisture from the powder affects transparency in the IR. The effect of post-treatments on such ceramics still needs to be studied. By releasing impurities, post-treatments could cracked the samples. On the other hand, a new two-step sintering process has shown an obvious improvement in the microstructure : for the same temperatures, the samples are denser and their microstructure finer than for a one-step treatment. In this study, at a temperature of 1200°C and under 70 MPa, the average grain diameter goes from 430 to 230 nm and the porosity rate from 9 to 3%. These differences have notable effects on the transparency of the samples in the IR. This transparency was then studied up to 1000°C on those samples after post-treatments. The reduction in transparency due to multi-phonon absorption is well observed. But owing to the high limit of the nanocomposite transparency window which goes up to 9 μm at room temperature, the band between 3 and 5 μm is only slightly affected. It begins to decrease after 750°C. The loss at 1000°C for a thickness of 2 mm and a wavelength of 5 μm is approximately 15%. The SPS and HIP parameters still need to be optimized by combining two-step sintering and one-step sintering at lower temperatures.

## REFERENCES

- [1] B. H. Kear, R. Sadangi, V. Shukla, T. Stefanik, et R. Gentilman, « Submicron-grained transparent yttria composites », in *Window and Dome Technologies and Materials IX*, International Society for Optics and Photonics, mai 2005, p. 227-233. doi: 10.1117/12.602333.
- [2] D. C. Harris *et al.*, « Properties of an Infrared-Transparent MgO:Y<sub>2</sub>O<sub>3</sub> Nanocomposite », *Journal of the American Ceramic Society*, vol. 96, n° 12, p. 3828-3835, 2013, doi: 10.1111/jace.12589.
- [3] L. Liu, K. Morita, T. S. Suzuki, et B.-N. Kim, « Evolution of microstructure, mechanical, and optical properties of Y<sub>2</sub>O<sub>3</sub>-MgO nanocomposites fabricated by high pressure spark plasma sintering », *Journal of the European Ceramic Society*, vol. 40, n° 13, p. 4547-4555, oct. 2020, doi: 10.1016/j.jeurceramsoc.2020.05.046.
- [4] M. E. Thomas, R. I. Joseph, et W. J. Tropsch, « Infrared transmission properties of sapphire, spinel, yttria, and ALON as a function of temperature and frequency », *Appl. Opt.*, vol. 27, n° 2, p. 239-245, janv. 1988, doi: 10.1364/AO.27.000239.
- [5] D. C. Harris, « Durable 3–5  $\mu$ m transmitting infrared window materials », *Infrared Physics & Technology*, vol. 39, n° 4, p. 185-201, juin 1998, doi: 10.1016/S1350-4495(98)00006-1.
- [6] N. Brard, J. Petit, N. Emery, N. Horezan, et S. Bach, « Control of the nanostructure of MgO–Y<sub>2</sub>O<sub>3</sub> composite ceramics using two-step sintering for high temperature mid infrared window applications », *Ceramics International*, févr. 2023, doi: 10.1016/j.ceramint.2023.02.187.
- [7] M.-Y. Chu, L. C. De Jonghe, M. K. F. Lin, et F. J. T. Lin, « Precoarsening to Improve Microstructure and Sintering of Powder Compacts », *Journal of the American Ceramic Society*, vol. 74, n° 11, p. 2902-2911, 1991, doi: 10.1111/j.1151-2916.1991.tb06861.x.
- [8] I.-W. Chen et X.-H. Wang, « Sintering dense nanocrystalline ceramics without final-stage grain growth », *Nature*, vol. 404, n° 6774, Art. n° 6774, mars 2000, doi: 10.1038/35004548.
- [9] H. J. Ma, W. K. Jung, S.-M. Yong, D. H. Choi, et D. K. Kim, « Microstructural freezing of highly NIR transparent Y<sub>2</sub>O<sub>3</sub>-MgO nanocomposite via pressure-assisted two-step sintering », *Journal of the European Ceramic Society*, vol. 39, n° 15, p. 4957-4964, déc. 2019, doi: 10.1016/j.jeurceramsoc.2019.07.029.
- [10] J. Xie, X. Mao, X. Li, B. Jiang, et L. Zhang, « Influence of moisture absorption on the synthesis and properties of Y<sub>2</sub>O<sub>3</sub>-MgO nanocomposites », *Ceramics International*, vol. 43, n° 1, Part A, p. 40-44, janv. 2017, doi: 10.1016/j.ceramint.2016.08.117.
- [11] S.-M. Yong *et al.*, « Study on carbon contamination and carboxylate group formation in Y<sub>2</sub>O<sub>3</sub>-MgO nanocomposites fabricated by spark plasma sintering », *Journal of the European Ceramic Society*, vol. 40, n° 3, p. 847-851, mars 2020, doi: 10.1016/j.jeurceramsoc.2019.10.035.
- [12] D. Jiang et A. K. Mukherjee, « The influence of oxygen vacancy on the optical transmission of an yttria–magnesia nanocomposite », *Scripta Materialia*, vol. 64, n° 12, p. 1095-1097, juin 2011, doi: 10.1016/j.scriptamat.2011.02.029.